materials

MDPI

Article

A Mathematical Model for the Electrical Resistivity of Cement Paste at Early Ages Considering the Partially Saturated State

Ye Tian [1], Xin Xu [1], Haodong Ji [1], Zushi Tian [1,*], Xianyu Jin [1], Nanguo Jin [1], Dongming Yan [1] and Shengwen Tang [2]

[1] Department of Civil Engineering and Architecture, Zhejiang University, Hangzhou 310058, China; cetianye@zju.edu.cn (Y.T); 21912155@zju.edu.cn (X.X.); jihd@zju.edu.cn (H.J.); xianyu@zju.eu.cn (X.J.); jinng@zju.edu.cn (N.J.); dmyan@zju.edu.cn (D.Y.)

[2] Department of Water Resources and Hydropower Engineering, Wuhan University, Wuhan 430070, China; tangsw@whu.edu.cn

* Correspondence: tianzs@connect.hku.hk; Tel.: +86-852-65825590

Received: 19 June 2020; Accepted: 22 July 2020; Published: 24 July 2020



Abstract: For cementitious materials, electrical resistivity is often used in the study of the cement hydration process at early age, as one of the few indicators that can be continuously and non-destructively monitored. Variation characteristics of resistivity are widely reported to interact with the early-age performance of cement paste, such as hydration kinetics parameters and setting time. However, there is no reasonable mathematical model to predict the resistivity at early ages, especially within the first 24 h, due to significant changes in the porosity and degree of saturation. In this work, a mathematical model was developed by considering the partially saturated state and density change of C-S-H (calcium silicate hydrate). To verify the model, two experimental methods were chosen, including the non-contact electrical resistivity test and isothermal calorimetry test. The hydration heat and resistivity of cement paste with a water–cement ratio of 0.35 and 0.45 were continuously monitored for 3 days. In the resistivity test, embedded temperature sensors were used to monitor the internal temperature and temperature correction was treated carefully in order to obtain accurate data. The test results prove that the mathematical model can accurately predict electrical resistivity and describe the saturation state of early-age cement pastes under sealed curing.

Keywords: cement paste; hydration degree; electrical resistivity; temperature; partially saturated

1. Introduction

The long-term performance of cementitious materials is determined by the early cement hydration process. It is well known that the cementitious material system is in an unsteady state and its macroscopic characteristics and microstructure change quickly at the early stage of hydration, especially within the first 48 h. Experimentally, there are only a few methods, which can accurately and continuously monitor the properties of cementitious materials by non-destructive means, such as isothermal calorimetry and electrical resistivity monitors. Isothermal calorimetry measures the hydration heat to characterize the hydration kinetics [1]. A detailed investigation suggested that the hydration process of cement paste can be divided into three phases, as the nucleation and growth reactions phase, boundary reactions phase and governs reactions phase [2,3]. In comparison to isothermal calorimetry, electrical resistivity monitors [4,5] are widely applied in the study of cement hydration because they reveal more information on the hydration mechanism [6–11] and microstructure evolution [12–15]. Based on the evolution of resistivity, the cement hydration process can be divided into four periods: dissolution, induction, accelerated and decelerated periods [6,7]. A series of investigations were

performed to further discuss the early-age properties of cementitious materials, such as the initial setting time [10,16,17], strength [11,17–19], hydration kinetic parameters [20,21] and chemical shrinkage [22,23], through electrical resistivity [24–28].

However, the existing cement hydration models do not explain the experimental data of isothermal calorimetry and electrical resistivity monitors at very early ages (less than 24 h), though they work well on a time scale of days and weeks. Firstly, it is difficult to characterize pore microstructure, pore solution distribution, and the degree of saturation at early age. Some common experimental techniques request dry samples, such as mercury intrusion porosimetry (MIP) and nitrogen adsorption isotherms (NAI). The process of hydration termination and drying may cause the damaging of pore structure, which is fragile at early age. Furthermore, the MIP technique always underestimates small pores in the cementitious material. In recent years, nuclear magnetic resonance (NMR), as a non-destructive monitoring technology, has been utilized to detect and distinguish capillary water gel water and air in cementitious materials [29,30]. On the basis of NMR data, an innovative analytical cement hydration model was proposed [31], which reveals the change of C-S-H gel density during hydration. The model is more reasonable and accurate in comparison with the widely-used Power's model [32] that assumes C-S-H gel density as a constant. Secondly, how the pore solution existing in different ways contributes to the overall conductivity needs to be further determined. Capillaries are generally considered to have good connectivity but the gel pore solution, which exists in the form of small isolated capillaries, micropores and interlayer space in both low density (LD) C-S-H gel and high density (HD) C-S-H gel [33,34], is separated by the gel chain. Finally, the cement paste is in a typical partially saturated state under sealed curing conditions, where water is consumed continuously by cement hydration. The degree of saturation has a significant effect on the overall resistivity [35,36].

In this work, a mathematical model was developed to predict the electrical resistivity of cement paste at early ages. In the model, physical and chemical changes of cement hydration at early ages were considered, including the partially saturated state and density change of C-S-H. The hydration heat and resistivity of cement paste with a water–cement ratio of 0.35 and 0.45 were continuously monitored for 3 days utilizing the non-contact electrical resistivity test and isothermal calorimetry test. After careful temperature correction, the test data were used to verify the rationality and accuracy of the model. It helps to better understand the relationship of the pore structure, moisture content, and resistivity of cement paste at early ages, especially within the first 48 h.

2. A Mathematical Model of Electrical Resistivity

2.1. Correction of Temperature Effect

Temperature affects two aspects of the resistivity of cement paste, electrical measurement and hydration [5,37]. The former is a single physical mechanism, that is, temperature influences the measured values of resistivity since the pore solution resistivity becomes lower at higher temperatures. The latter is a chemical mechanism, that is, the hydration rate of cementitious materials increases as the reaction temperature rises.

For the effect of temperature on electrical measurement, previous investigations [38–40] used a linear equation with the temperature correction coefficient for cementitious materials covering a range of 0.018 to 0.025 $°C^{-1}$. The value is close to the temperature correction coefficient of pure water and alkaline solutions [41]. However more recently, investigations [4,42–44] suggested the use of the activation-energy-based formula to correct the temperature effect presented in Equation (1):

$$\rho_{T_0} = \rho_T \cdot exp\left[\frac{E_{a-cond}}{R}\left(\frac{1}{T} - \frac{1}{T_0}\right)\right], \quad (1)$$

where $E_{a\text{-}cond}$ is the activation energy of conduction, R is the gas constant and the value is 8.31 J/(K·mol). Previous investigations reported different values for the activation energy of conduction of cementitious materials including 18.7, 19.9–23.4, 16.8–21.2, 16–30 kJ/mol [4,5,43,44]. Moreover, the activation energy

of conduction is related to relative humidity and curing conditions [5,45]. Therefore, the value of 23.4 kJ/mol measured in sealed conditions [5] was chosen in this research.

For the effect of temperature on hydration, the equivalent maturity theory is usually used to correct the resistivity to the value at the reference temperature. According to the theory, time t at the variable temperature T of actual reaction corresponds to the equivalent maturity age t_{eq} at reference temperature T_{ref}. That means the hydration degree, as well as the resistivity, at t is equal to that at t_{eq} under a constant reference temperature T_{ref}. Therefore, the following equation can be given as:

$$\rho_{T_{ref}}\left(t_{eq}\right) = \rho_{T_{var}}(t), \tag{2}$$

where $\rho_{T_{ref}}$ is the resistivity of cement paste under reference temperature T_{ref} at the equivalent maturity age t_{eq}, $\rho_{T_{var}}$ is the resistivity at the variable temperature T of actual reaction at the actual maturity age t. The equivalent maturity age t_{eq} can be calculated by the Arrhenius equation [46,47], as:

$$t_{eq} = \int_0^t exp\left[\frac{E_{a-hyd}}{R}\left(\frac{1}{T_{ref}} - \frac{1}{T(t)}\right)\right]dt, \tag{3}$$

where $E_{a\text{-}hyd}$ is the activation energy of hydration reaction. It should be noted that the equivalent time is affected by the temperature history changing with time rather than the temperature at a certain moment or the average temperature. For ordinary Portland cement, the activation energy is generally obtained within a narrow range from 40 to 45 kJ/mol, as recommended by ASTM C 1074. In this study, the value of 40.5 kJ/mol was adopted [48].

2.2. A Mathematical Model of Resistivity

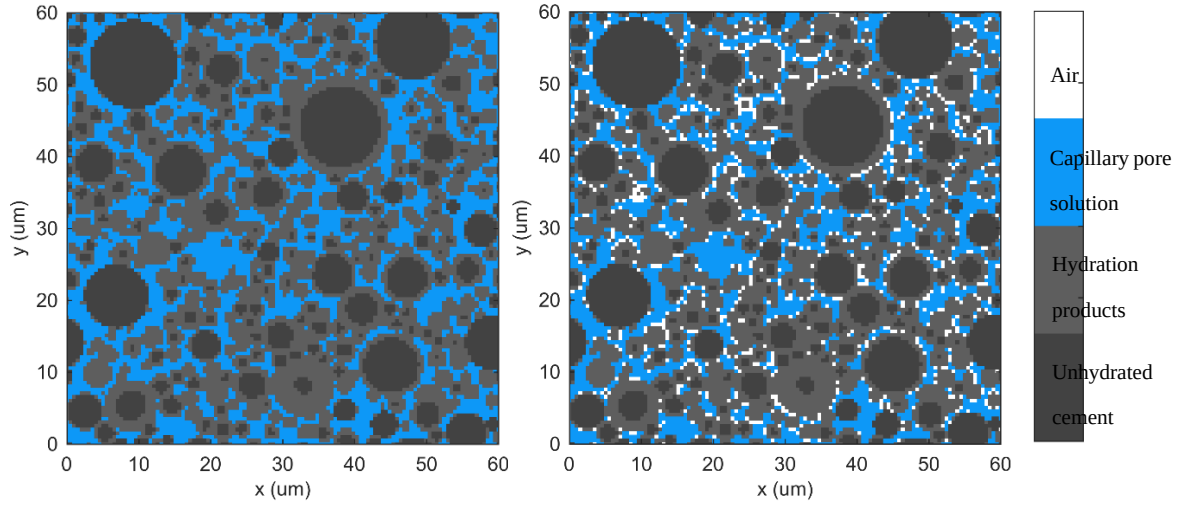
The relationship of the overall resistivity of composite materials and the resistivity of each phase can be described by the general effective media (GEM) model [49,50], and be calculated by the following equations for cementitious systems [12], as:

$$\varphi_{low} = \left[(1-\varphi_c)F^{-\frac{1}{m}} - \varphi_c\right]\cdot\left(\frac{M^{\frac{1}{m}} - F^{-\frac{1}{m}}}{M^{\frac{1}{m}} - 1}\right), \tag{4}$$

$$F = \frac{\rho}{\rho_{low}},\ \ M = \frac{\rho_{high}}{\rho_{low}}, \tag{5}$$

where ρ is the overall resistivity of cement paste, ρ_{low} is the resistivity of the low resistivity phase, ρ_{high} is the resistivity of the high resistivity phase, φ_{low} is the volume fraction of the low resistivity phase, F is the resistivity formation factor, M is the magnification coefficient between ρ_{high} and ρ_{low}; φ_c is the percolation threshold, m is the critical exponent. This model works well to characterize various properties in the saturated cementitious system, such as the diffusion coefficient [51], water permeability [52] and resistivity [12–14].

However, porosity cannot be considered as the low resistivity phase for the partially saturated system, as is shown in Figure 1. Cement paste is a complex compound consisting of liquid, gas and solid phases, including unhydrated cement particles and hydration products consisting of calcium hydroxide (CH) and C-S-H gel. Among these phases, only the capillary solution and C-S-H gel are electrically conductive but C-S-H gel has limited contribution to conductivity because its resistivity is 400 times that of pore solution [12]. It should be noted that not all pore solutions have the same contribution to conductivity. The gel pore solution, which exists in the form of small isolated capillaries, micropores and interlayer space in C-S-H gel [33,34], has limited contribution to conductivity. Because the migration of ions is blocked by the gel chain, which is the main reason why C-S-H gel has a hundred times higher resistivity than pore solution. On the contrary, the capillary pores are believed to be interconnected where they can migrate freely. Therefore, it is more reasonable to determine that the capillary solution is the main conductive phase in cementitious systems.



(**a**) (**b**)

Figure 1. Schematic diagram of cement paste microstructure: (**a**) Saturated, (**b**) Unsaturated.

Another problem is how to determine the volume fraction of the capillary pore solution. In this study, the analytical cement hydration model [31] based on an NMR experiment was used. Comparing with the widely-used Power's model [32], the model functions on the basis of continuous non-destructive monitoring of water in cement paste during hydration, and considers the density change of C-S-H. According to the analytical model, the volume fraction of gel and capillary pores (water-filled) can be calculated from Equations (6) and (7):

$$\varphi_{gpor} = \begin{cases} 0 & 0 \le \alpha \le \alpha_{I-II} \\ \frac{-0.799(w/c)^2+4.824(w/c)\cdot\alpha-0.793\alpha^2}{(1+3.185w/c)(0.864w/c+1.278\alpha)} & \alpha_{I-II} \le \alpha \le \alpha_{II-III} \\ \frac{3.185w/c-0.755\alpha}{1+3.185w/c} \ge 0 & \alpha_{II-III} \le \alpha \le 1 \end{cases}, \quad (6)$$

$$\varphi_{cpor} = \frac{3.185w/c - 0.755\alpha}{1 + 3.185w/c} - \varphi_{gpor} \ge 0, \quad (7)$$

where w/c is the water to cement ratio of cement paste, α is the hydration degree of cement paste, φ_{cpor} is the volume fraction of capillary pore solution, φ_{gpor} is the volume fraction of gel pore solution, α_{I-II} is the hydration degree at the transition from hydration regime I to II and α_{II-III} is the hydration degree at the transition from hydration regime II to III [31]. α_{I-II} and α_{II-III} are related with w/c and can be calculated from:

$$\alpha_{I-II} = 0.170w/c,\ \alpha_{II-III} = 2.022w/c \quad (8)$$

From the analysis above, the capillary pore solution was regarded as the unique low-resistivity phase. According to the original definition in the general effective media equation, φ_{low} in Equation (4) should be substituted into Equation (7) as φ_{cpor}. Combining Equation (4), Equation (5) and Equation (7) together, the relationship between hydration degree α and resistivity ρ can be furtherly deduced by following equation.

$$\varphi_{cpor} = \frac{3.185w/c - 0.755\alpha}{1 + 3.185w/c} - \varphi_{gpor} = \left[(1-\varphi_c)\left(\frac{\rho}{\rho_{liq}}\right)^{-\frac{1}{m}} - \varphi_c\right] \cdot \left(\frac{M^{\frac{1}{m}} - \left(\frac{\rho}{\rho_{liq}}\right)^{-\frac{1}{m}}}{M^{\frac{1}{m}} - 1}\right) \quad (9)$$

Pore solution resistivity is constantly changing during cement hydration. The value is related to the initial alkali content, the water-cement ratio, the cement hydration age and the curing conditions [5,7,53,54]. In this study, the pore solution resistivity was calculated by an online tool

developed by Bentz [55–57]. This model predicts the pore solution resistivity of cement paste under sealed conditions using the water–cement ratio, the alkali content (Na_2O, K_2O) and hydration degree. According to this model, the relationship between resistivity and hydration degree is linear and can be described by the following equations:

$$\rho_{cpor} = \begin{cases} -0.0695a + 0.1634 & w/c = 0.50 \\ -0.0701a + 0.1480 & w/c = 0.45 \\ -0.0708a + 0.1335 & w/c = 0.40 \\ -0.0717a + 0.1185 & w/c = 0.35 \\ -0.0731a + 0.1034 & w/c = 0.30 \end{cases}. \quad (10)$$

3. Experiment

3.1. Materials and Sample Preparation

ASTM Type I ordinary Portland cement with a specific gravity of 3.15 and specific surface area of 350 m^2/kg was used in the work. The mineral composition of ordinary Portland cement tested by XRF (X-ray fluorescence spectrometer) is listed in Table 1. The ultimate hydration heat of cement is 457 kJ/kg according to the mass fraction and the hydration heat of each mineral content. Deionized water was used in the non-contact electrical resistivity measurement and isothermal calorimetry. Two kinds of cement pastes were prepared with *w/c* ratios of 0.35 and 0.45, which were denoted as P35 and P45, respectively.

Table 1. Mineral composition and hydration heat of cement.

Mineral Composition	C_3S	C_2S	C_3A	C_4AF	Gypsum	K_2O	Na_2O	Total
Mass fraction (%)	65.78	7.75	6.94	8.64	6.99	0.68	0.13	97.91
Hydration heat (kJ/kg)	517	262	867	418				457

3.2. Non-Contact Electrical Resistivity Measurement

The resistivity of the cement paste was obtained by a non-contact electrical resistivity measurement device. Cement and water were put into the dedicated mixer, and slowly stirred for 120 s, paused for 5 s and quickly stirred for 120 s. After mixing, 2 L of the fresh mixtures were cast in a ring-shaped mold immediately and then the mold was vibrated gently to exclude bubbles out of the paste. Afterwards, the mold was covered by a plastic lid and sealed with Vaseline to prevent evaporation of water. In this research, two temperature sensors were embedded in the specimen symmetrically to record the internal temperature of the cement paste. Moreover, another two temperature sensors were employed to monitor the ambient temperature. The data were transferred to a computer and recorded once a minute. After measurement for 72 h, the specimen was taken out of the mold. Then the height of the specimen was measured to revise the electrical resistivity measurement results. For P45, the ambient temperature was maintained at 18, 23 and 28 °C during the measurement. For P35, the resistivity was measured under a temperature of 18 °C. The non-contact electrical resistivity device can be seen in Figure 2.

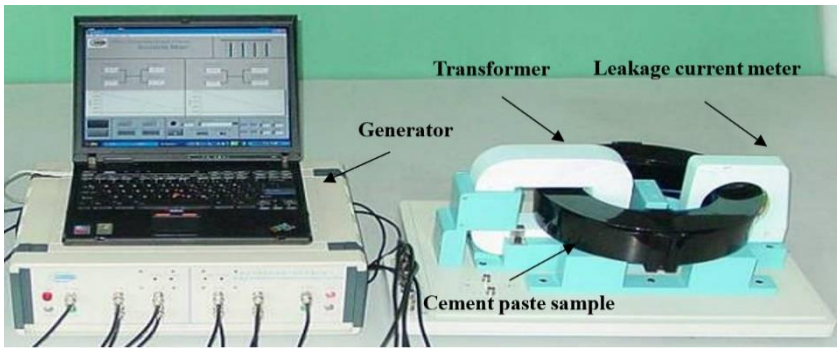


Figure 2. Non-contact electrical resistivity device.

3.3. Isothermal Calorimetry Experiment

During the isothermal calorimetry experiment, Portland cement and deionized water were put into an admix ampoule and fully mixed by a stirrer. Then the accumulated hydration heat and heat flow of cement paste were measured using a TAM Air 08 Isothermal Calorimeter, which was manufactured by TA Instruments. The isothermal calorimetry experiment was conducted for 72 h. The temperature of the cement paste sample was strictly controlled at 20 °C during the experiment process.

4. Experiment Results and Discussion

4.1. Hydration Degree

In this research, the hydration degree of cement paste was represented as the ratio of released hydration heat to the ultimate hydration heat calculated according to the chemical composition of cement, which is listed in Table 1. Moreover, the hydration degree variation rate was calculated from the heat flow divided by the ultimate hydration heat. The experiment results are shown in Figure 3.

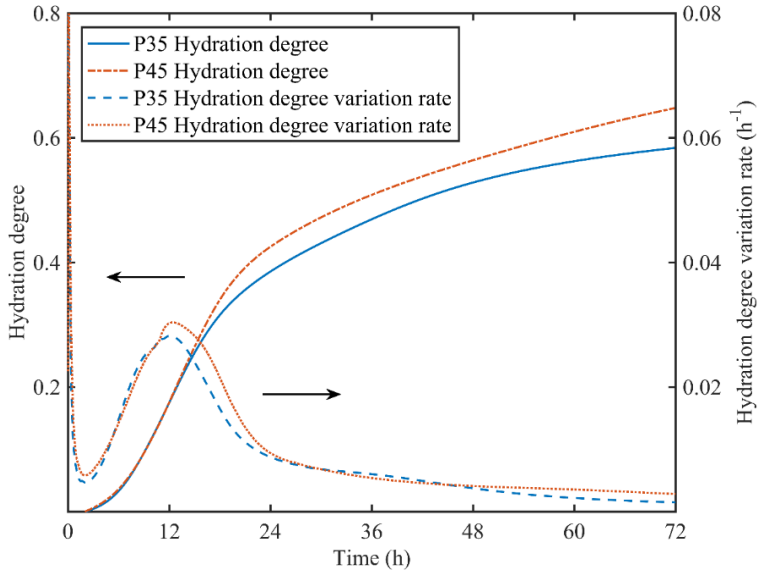


Figure 3. Hydration degrees and hydration degree variation rates of P35 and P45.

In the isothermal calorimetry tests, the volume of the cement paste sample in the admix ampoule was very small, and the generated hydration heat was released to the environment rapidly. The reaction temperature of the sample maintained under the control temperature during the whole experiment process as no hydration heat was absorbed by the sample. Because the cement particles were all in sufficient contact with water at the beginning of hydration period, the hydration degree of P35 and P45 showed no obvious differences from 0 to 12 h, which can be seen in Figure 3. While afterwards,

the hydration degree of P45 was higher than that of P35 due to a higher water to cement ratio. At 72 h, the hydration degrees of P45 and P35 were 0.66 and 0.58, respectively. This phenomenon is in agreement with previous research as a higher water to cement ratio means a more sufficient supply of water during the hydration process [58].

From the curve of hydration degree variation rate, the hydration process of cement pastes can be divided into three periods. In the period of 0–2 h, the heat flow is released by wetting the cement particle and the dissolution of cement particle. The decreasing hydration rate corresponds to the decrease in dissolution rate. From 2 to 24 h, the hydration rate has an evident peak corresponding to nucleation and growth reactions and phase boundary interaction reactions. Finally, the hydration process will come to an end gradually with the consumption of water. Simultaneously, the hydration rate is primarily governed by diffusion and drops close to zero from 24 to 72 h [2].

4.2. Electrical Resistivity

For non-contact electrical resistivity measurement, the generated hydration heat can't be released to the environment immediately and part of hydration heat will accumulate inside the sample. Although, the environment temperature for electrical resistivity measurement was also controlled as a constant. There was a temperature gradient from the center to the surface of the specimen. The internal temperature of P45 under different environmental conditions is shown in Figure 4.

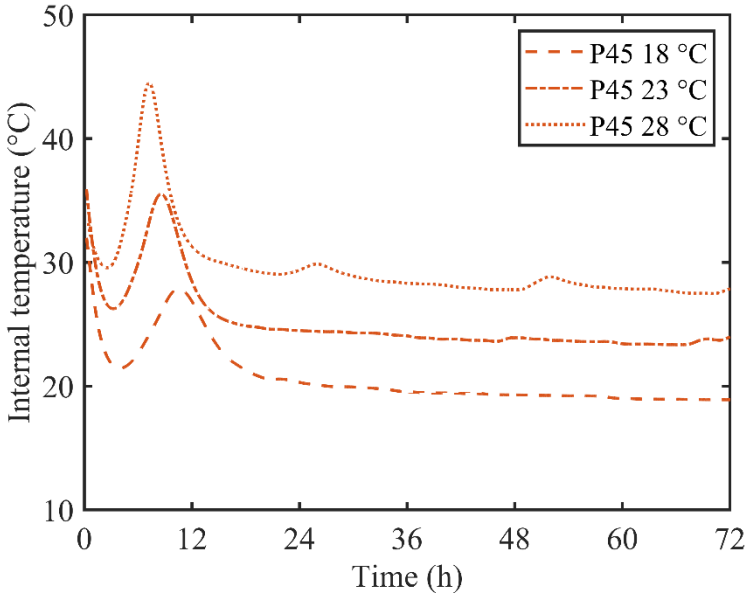


Figure 4. Internal temperature of P45 under different ambient temperatures.

The internal temperature actually reflects the hydration heat accumulated within the specimen during the electrical resistivity measurement. As a result, the internal temperature and the hydration degree developed similar trends. As shown in Figure 4, the internal temperature also decreased rapidly at the early age, and a temperature peak appeared in the first 24 h, followed by a gradual reduction which indicates the final dissipation of hydration heat. The internal temperature achieved its highest value as 44.6, 35.6 and 27.9 °C when the environmental temperature was 28, 23 and 18 °C, respectively. At the same time, the internal temperature reached its peak value at 7.3, 8.6 and 10.5 h for environment temperatures of 28, 23 and 18 °C, respectively. It is understandable that, as indicated in Figure 4, the high environmental temperature will promote the hydration process of cement paste, which, accordingly, will release lots of hydration heat quickly.

As mentioned previously, temperature can affect the resistivity of cement paste in two ways. The influence of temperature on ionic movability can be corrected utilizing a temperature correction formula. However, the influence on hydration reaction rate can't be fully corrected from Equation (1).

As a result, the resistivity and resistivity variation rate curves are still highly correlated with temperature. To essentially clarify the influence on hydration reaction rate, the completely and partly corrected electrical resistivity, as well as the resistivity variation rate, are shown in Figures 5 and 6.

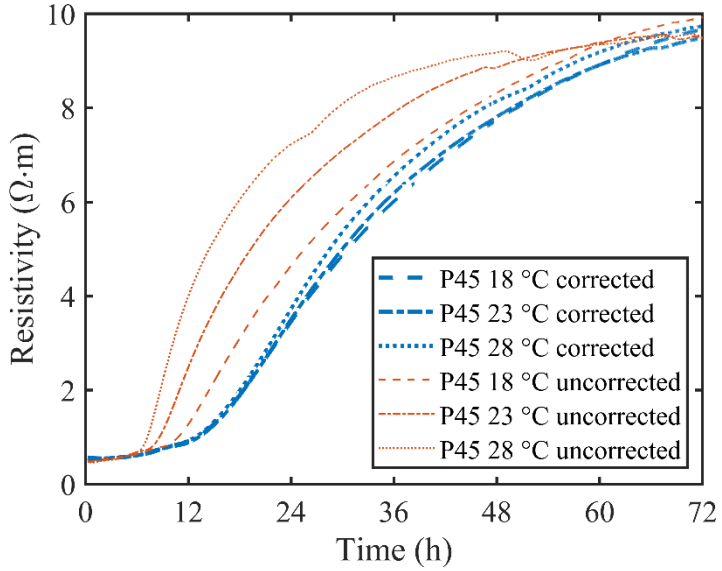


Figure 5. Completely and partly corrected electrical resistivity of P45 under different ambient temperatures.

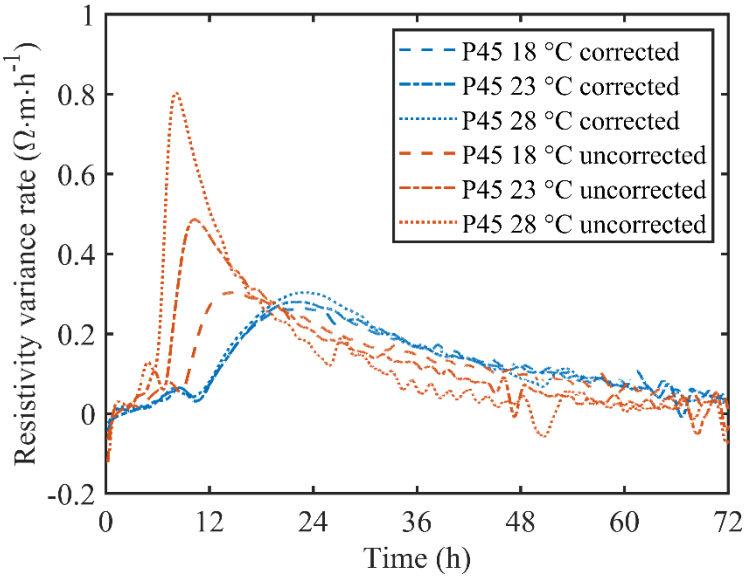


Figure 6. Completely and partly corrected resistivity variation rate of P45 under different ambient temperatures.

Although the temperature influence on ionic movability was corrected with Equation (1), the temperature had already affected the hydration process of cement paste. As shown in Figure 5, the partly corrected resistivity curves of P45 under different environmental temperature conditions are quite different from each other. A high environment temperature corresponds to a high corrected electrical resistivity, indicating a dense microstructure and a high hydration degree. This phenomenon can be furtherly explained by the development of resistivity variation rate, as shown in Figure 6. The resistivity variation rate curves show a similar trend to the internal temperature of P45. A peak can be also seen in each resistivity variation rate curve under different environmental temperatures. Moreover, a high temperature achieved a high peak value, which indicates that the electrical resistivity

evolved rapidly under high temperature. Furthermore, the resistivity variation rate reached the peak quickly in the high temperature environment. The experimental results demonstrate that the influence of temperature hydration reaction rate affects the resistivity of cement paste significantly, which can't be ignored, especially in the early stage of hydration. Therefore, this temperature influence was corrected based on equivalent age theory by substituting partly corrected electrical resistivity and internal temperature history into Equation (2).

After a complete correction, the electrical resistivity was standardized into the equivalent value in the isothermal conditions of 20 °C. Then the standardized resistivity variation rate was calculated from the derivative of the standardized resistivity with respect to time. As shown in Figure 5, the completely corrected resistivity curves of P45 at different environment temperatures were almost coincident with each other, and the resistivity at 72 h was 10.28, 9.76 and 9.60 Ω·m corresponding to 28, 23 and 18 °C, respectively. Data analysis indicated that the relative standard deviation of the resistivity at 72 h was 2.9% and the maximal relative deviation was 4%. Meanwhile, in Figure 6, the corrected resistivity variation rate curves are well coincident, and the peaks appear at 23.2, 22.9 and 22.6 h in specified values as 0.312, 0.280 and 0.259 $\Omega \cdot m \cdot h^{-1}$, accordingly. The peak value and the appearance time of all resistivity variation rate curves were both very close to each other, implying that the influence of temperature on hydration reaction rate can be corrected off by Equation (2) based on the equivalent age theory.

It can be concluded from Figures 5 and 6 that a standardized treatment of measured resistivity is very necessary before further data analysis. Nevertheless, the temperature influence on hydration reaction rate is entirely neglected in some previous studies. It would cause negative consequences in two aspects: firstly, the partly corrected electrical resistivity cannot reflect the internal temperature history of samples. Strictly speaking, all the electrical resistivity results measured by non-contact resistivity devices are performed under different temperatures as different cementitious materials have unique hydration processes. Although the partly corrected resistivity characterizes the microstructure properties of cementitious materials, the essential properties of electrical resistivity are covered by internal temperature. Secondly, ignoring the temperature influence on hydration reaction rate restricts the application of a non-contact electrical resistivity measurement. It is irrational to compare the incompletely processed resistivity data with other experiment results, such as those obtained from isothermal calorimetry. Although the resistivity measurement and isothermal calorimetry test are both employed to assess the hydration process, the key time points have no similarity even if the two tests are conducted under the same environment temperature. As a result, it is the isothermal calorimetry test that is widely accepted and utilized to estimate the hydration degree of cementitious materials rather than the electrical resistivity measurement.

4.3. Verification of the Mathematical Model

In this study, the hydration degree was tested by isothermal calorimetry tests and then the volume fraction of capillary pore solution can be calculated by Equations (6) and (7). The electrical resistivity was measured by the non-contact electrical resistivity device and the temperature effect on resistivity was corrected carefully. The formation factor was calculated based on the corrected electrical resistivity by Equation (5). The parameters, including percolation threshold φ_c, exponent parameter m, and magnification coefficient M, in the general effective media equation needed to be determined. The percolation threshold was from 0.17 to 0.20 [59–63] for cement paste and independent of the initial porosity or *w/c* ratio, which was selected as 0.18 in this study [64,65]. The exponent parameter m in the GEM equation was related to the geometry of the low resistivity phase with a theoretical value of 2 for cement paste [65]. Although this parameter varies from 1.4 to 2.46 for composites [49,66], it has limited effect on the calculation results [12]. In this study, the exponent parameter was limited as 1.8–2.2. The magnification coefficient was the electrical resistivity ratio of the high resistivity phase to the low resistivity phase, which varied with material and age. Garboczi and Bentz [65] indicated that

the resistivity of C-S-H was about 400 times as much as that of pore solution (M = 400). While other researchers reported relatively low values of 100 [63] and 133.3 [67].

In this investigation, the magnification coefficient was determined by fitting the data points of the volume fraction of capillary pore solution and the formation factor, as shown in Figure 7. Table 2 shows the results of 262.1 for P35 and 174.2 for P45, which was smaller than that of the C-S-H gel [65]. It is reasonable because the parameters were obtained based on test results during the first 72 h when C-S-H gel has a looser pore structure and higher electrical conductivity compared with the cement paste at mature age. P35 has a greater magnification coefficient than that of P45 because of a higher volume fraction of unhydrated cement particles.

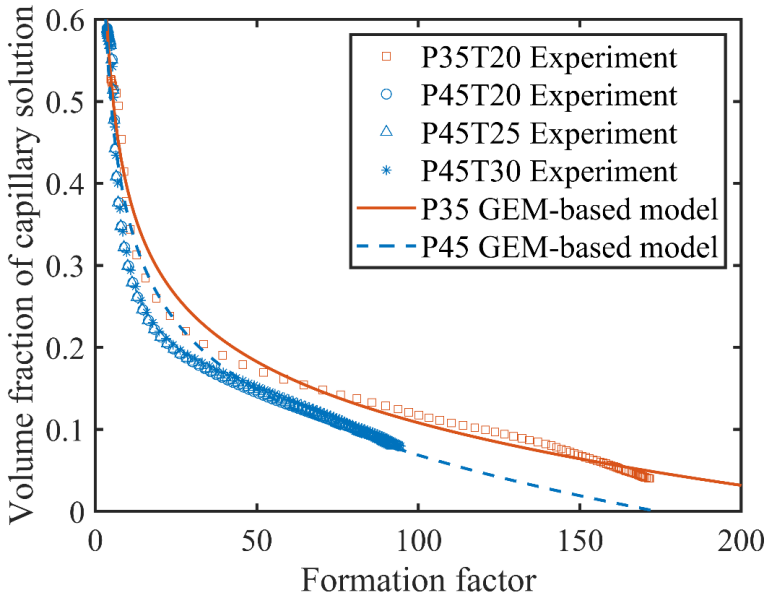


Figure 7. Curve fitting between volume fraction of capillary pore solution and formation factor.

Table 2. The parameters of the general effective media (GEM) based model.

Mix	ϕc	M	m	R2
P35	0.18	262.1	2.184	0.9899
P45	0.18	174.2	2.003	0.9721

Once the parameters in the general effective media equation were determined, the electrical resistivity could be predicted based on the hydration degree from isothermal calorimetry tests. In Figure 8, the predicted and measured resistivity have a good agreement overall for both P35 and P45 though there are deviations in several parts. The possible reason is that exponent parameter m and magnification coefficient M are assumed as constant in the GEM model. However, at the early hydration process, both parameters may change with evolution in the chemical composition and pore microstructure. During the dissolution stage (first 2 h) or before final setting time, the mathematical model still can provide accurate prediction results. It proves that the mathematical model can quantitatively describe the relationship between the hydration degree and electrical resistivity of cement paste, especially in the early stages of cement hydration.

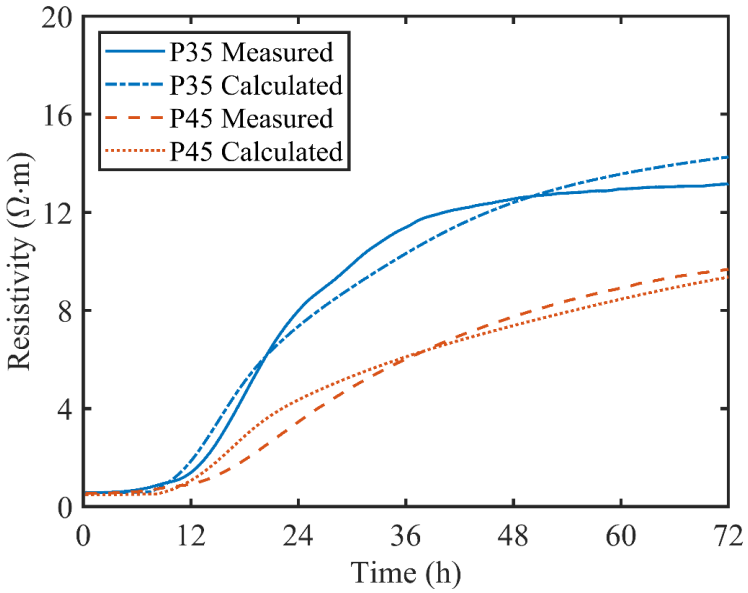


Figure 8. Comparison between the measured resistivity and the calculated resistivity.

5. Conclusions

In this work, a mathematical model was developed by considering the partially saturated state and density change of C-S-H and was well verified by the non-contact electrical resistivity test and isothermal calorimetry test. This model describes the changes in porosity and saturation state of cement compounds and the relationship between hydration degree and electrical resistivity during hydration. It has advantages in predicting the electrical resistivity of cementitious material at early age, especially for the first 48 h. The temperature correction based on the real-time temperature curve, measured by the embed temperature sensor, is recommended in resistivity measurement. This method is suitable for obtaining accurate electrical resistivity data in the early age of cement hydration.

Author Contributions: Conceptualization, Y.T., X.X. and Z.T.; methodology, Y.T., X.X. and H.J.; software, Y.T. and Z.T.; validation, Y.T., X.X. and Z.T.; formal analysis, X.X. and Z.T.; investigation, Y.T. and H.J.; resources, Y.T., X.X. and Z.T.; data curation, Y.T., H.J. and Z.T.; writing—original draft preparation, X.X. and Z.T.; writing—review and editing, Y.T. and Z.T.; visualization H.J.; supervision, Y.T.; project administration, Y.T.; funding acquisition, X.J., N.J., D.Y. and S.T. All authors have read and agreed to the published version of the manuscript.

Funding: This research was financially supported by the National Key Basic Research Program of China (973 program) (Grant No. 2015CB655103) and the National Natural Science Foundation of China (Grant No. 51578497, 51378012).

Conflicts of Interest: The authors declare no conflict of interest. The funders had no role in the design of the study; in the collection, analyses, or interpretation of data; in the writing of the manuscript, or in the decision to publish the results.

References

1. Pang, X.; Bentz, D.P.; Meyer, C.; Funkhouser, G.P.; Darbe, R. A comparison study of Portland cement hydration kinetics as measured by chemical shrinkage and isothermal calorimetry. *Cem. Concr. Compos.* **2013**, *39*, 23–32. [CrossRef]
2. Dabiĉ, P.; Krstuloviĉ, R.; Rušiĉ, D. A new approach in mathematical modelling of cement hydration development. *Cem. Concr. Res.* **2000**, *30*, 1017–1021. [CrossRef]
3. Yin, B.; Kang, T.; Kang, J.; Chen, Y.; Wu, L.; Du, M. Investigation of the hydration kinetics and microstructure formation mechanism of fresh fly ash cemented filling materials based on hydration heat and volume resistivity characteristics. *Appl. Clay Sci.* **2018**, *166*, 146–158. [CrossRef]
4. Rajabipour, F. Insitu Electrical Sensing and Material Health Monitoring in Concrete Structures. Ph.D. Thesis, Purdue University, West Lafayette, IN, USA, 2006.

5. Spragg, R.; Villani, C.; Snyder, K.; Bentz, D.; Bullard, J.W.; Weiss, J. Factors that influence electrical resistivity measurements in cementitious systems. *Transp. Res. Rec.* **2013**, *2342*, 90–98. [CrossRef]
6. Li, Z.; Wei, X.; Li, W. Preliminary interpretation of portland cement hydration process using resistivity measurements. *Mater. J.* **2003**, *100*, 253–257. [CrossRef]
7. Xiao, L.; Li, Z. Early-age hydration of fresh concrete monitored by non-contact electrical resistivity measurement. *Cem. Concr. Res.* **2008**, *38*, 312–319. [CrossRef]
8. Bu, Y.; Weiss, J. The influence of alkali content on the electrical resistivity and transport properties of cementitious materials. *Cem. Concr. Compos.* **2014**, *51*, 49–58. [CrossRef]
9. Zuo, Y.; Zi, J.; Wei, X. Hydration of cement with retarder characterized via electrical resistivity measurements and computer simulation. *Constr. Build. Mater.* **2014**, *53*, 411–418. [CrossRef]
10. Li, W.; Zhu, X.; Hong, J.; She, W.; Wang, P.; Zuo, W. Effect of anionic emulsifier on cement hydration and its interaction mechanism. *Constr. Build. Mater.* **2015**, *93*, 1003–1011. [CrossRef]
11. Farzanian, K.; Teixeira, K.P.; Rocha, I.P.; De Sa Carneiro, L.; Ghahremaninezhad, A. The mechanical strength, degree of hydration, and electrical resistivity of cement pastes modified with superabsorbent polymers. *Constr. Build. Mater.* **2016**, *109*, 156–165. [CrossRef]
12. Zhang, J.; Li, Z. Application of GEM Equation in microstructure characterization of cement-based materials. *J. Mater. Civ. Eng.* **2009**, *21*, 648–656. [CrossRef]
13. Liu, Z.; Zhang, Y.; Jiang, Q. Continuous tracking of the relationship between resistivity and pore structure of cement pastes. *Constr. Build. Mater.* **2014**, *53*, 26–31. [CrossRef]
14. Liu, Z.; Zhang, Y.; Liu, L.; Jiang, Q. An analytical model for determining the relative electrical resistivity of cement paste and C–S–H gel. *Constr. Build. Mater.* **2013**, *48*, 647–655. [CrossRef]
15. Tang, S.W.; Li, Z.J.; Chen, E.; Shao, H.Y. Impedance measurement to characterize the pore structure in Portland cement paste. *Constr. Build. Mater.* **2014**, *51*, 106–112. [CrossRef]
16. Liao, Y.; Wei, X. Penetration resistance and electrical resistivity of cement paste with superplasticizer. *Mater. Struct.* **2014**, *47*, 563–570. [CrossRef]
17. Dong, B.; Zhang, J.; Wang, Y.; Fang, G.; Liu, Y.; Xing, F. Evolutionary trace for early hydration of cement paste using electrical resistivity method. *Constr. Build. Mater.* **2016**, *119*, 16–20. [CrossRef]
18. Xiao, L.; Wei, X. Early age compressive strength of pastes by electrical resistivity method and maturity method. *J. Wuhan Univ. Technol. Mater. Sci. Ed.* **2011**, *26*, 983–989. [CrossRef]
19. Wei, X.; Xiao, L.; Li, Z. Prediction of standard compressive strength of cement by the electrical resistivity measurement. *Constr. Build. Mater.* **2012**, *31*, 341–346. [CrossRef]
20. Wei, X.; Xiao, L. Kinetics parameters of cement hydration by electrical resistivity measurement and calorimetry. *Adv. Cem. Res.* **2014**, *26*, 187–193. [CrossRef]
21. Wei, X.; Xiao, L. Effect of temperature on the electrical resistivity of Portland cement pastes. *Adv. Cem. Res.* **2012**, *24*, 69–76. [CrossRef]
22. Liao, Y.; Wei, X. Relationship between chemical shrinkage and electrical resistivity for cement pastes at early age. *J. Mater. Civ. Eng.* **2014**, *26*, 384–387. [CrossRef]
23. Zuo, Y.; Wei, X. Relations among electrical resistivity, chemical and autogenous shrinkage of cement pastes. *Adv. Cem. Res.* **2015**, *27*, 175–183. [CrossRef]
24. Tang, S.W.; Cai, X.H.; He, Z.; Shao, H.Y.; Li, Z.J.; Chen, E. Hydration process of fly ash blended cement pastes by impedance measurement. *Constr. Build. Mater.* **2016**, *113*, 939–950. [CrossRef]
25. Tang, S.W.; Li, Z.J.; Shao, H.Y.; Chen, E. Characterization of early-age hydration process of cement pastes based on impedance measurement. *Constr. Build. Mater.* **2014**, *68*, 491–500. [CrossRef]
26. Tang, S.W.; Cai, X.H.; He, Z.; Zhou, W.; Shao, H.Y.; Li, Z.J.; Wu, T.; Chen, E. The review of early hydration of cement-based materials by electrical methods. *Constr. Build. Mater.* **2017**, *146*, 15–29. [CrossRef]
27. Tang, S.W.; Cai, X.H.; Zhou, W.; Shao, H.Y.; He, Z.; Li, Z.J.; Ji, W.M.; Chen, E. In-situ and continuous monitoring of pore evolution of calcium sulfoaluminate cement at early age by electrical impedance measurement. *Constr. Build. Mater.* **2016**, *117*, 8–19. [CrossRef]
28. Cai, R.; He, Z.; Tang, S.; Wu, T.; Chen, E. The early hydration of metakaolin blended cements by non-contact impedance measurement. *Cem. Concr. Compos.* **2018**, *92*, 70–81. [CrossRef]
29. Valori, A.; McDonald, P.J.; Scrivener, K.L. The morphology of C–S–H: Lessons from 1H nuclear magnetic resonance relaxometry. *Cem. Concr. Res.* **2013**, *49*, 65–81. [CrossRef]

30. Muller, A.C.A.; Scrivener, K.L.; Gajewicz, A.M.; McDonald, P.J. Use of bench-top NMR to measure the density, composition and desorption isotherm of C–S–H in cement paste. *Microporous Mesoporous Mater.* **2013**, *178*, 99–103. [CrossRef]
31. Königsberger, M.; Hellmich, C.; Pichler, B. Densification of C-S-H is mainly driven by available precipitation space, as quantified through an analytical cement hydration model based on NMR data. *Cem. Concr. Res.* **2016**, *88*, 170–183. [CrossRef]
32. Hansen, T.C. Physical structure of hardened cement paste. A classical approach. *Mater. Struct.* **1986**, *19*, 423–436. [CrossRef]
33. Mindess, S.; Young, J.F.; Darwin, D. *Concrete*; Prentice Hall: Upper Saddle River, NJ, USA, 2003; ISBN 978-0-13-064632-3.
34. Jennings, H.M. Colloid model of C−S−H and implications to the problem of creep and shrinkage. *Mater. Struct.* **2004**, *37*, 59–70. [CrossRef]
35. Weiss, J.; Snyder, K.; Bullard, J.; Bentz, D. Using a saturation function to interpret the electrical properties of partially saturated concrete. *J. Mater. Civ. Eng.* **2013**, *25*, 1097–1106. [CrossRef]
36. Rajabipour, F.; Weiss, J. Electrical conductivity of drying cement paste. *Mater. Struct.* **2007**, *40*, 1143–1160. [CrossRef]
37. Spragg, R.; Bu, Y.; Snyder, K.; Bentz, D.; Weiss, J. *Electrical Testing of Cement-Based Materials: Role of Testing Techniques, Sample Conditioning*; Purdue University: West Lafayette, IN, USA, 2013.
38. Spencer, R.W. Measurement of the moisture content of concrete. *J. Proc.* **1937**, *34*, 45–64.
39. Whittington, H.W.; McCarter, J.; Forde, M.C. The conduction of electricity through concrete. *Mag. Concr. Res.* **1981**, *33*, 48–60. [CrossRef]
40. Buenfeld, N.R.; Newman, J.B. The permeability of concrete in a marine environment. *Mag. Concr. Res.* **1984**, *36*, 67–80. [CrossRef]
41. Barron, J.J.; Ashton, C. The effect of temperature on conductivity measurement. *TSP* **2005**, *7*, 1–5.
42. Rajabipour, F.; Weiss, J. Linking Health monitoring in concrete structures with durability performance simulations. In Proceedings of the Structure Congress, St. Louis, MO, USA, 18–21 May 2006; American Society of Civil Engineers: Reston, VA, USA, 2006; pp. 1–10.
43. McCarter, W.J.; Starrs, G.; Chrisp, T.M. Electrical conductivity, diffusion, and permeability of Portland cement-based mortars. *Cem. Concr. Res.* **2000**, *30*, 1395–1400. [CrossRef]
44. Sant, G.; Rajabipour, F.; Weiss, W. The influence of temperature on electrical conductivity measurements and maturity predictions in cementitious materials during hydration. *Indian Concr. J.* **2008**, *82*, 7–16.
45. Zaccardi, Y.A.V.; García, J.F.; Huélamo, P.; Maio, Á.A.D. Influence of temperature and humidity on Portland cement mortar resistivity monitored with inner sensors. *Mater. Cor.* **2009**, *60*, 294–299. [CrossRef]
46. Carino, N.J.; Lew, H.S. *The Maturity Method: From Theory to Application*; American Society of Civil Engineers: Reston, VN, USA, 2001; pp. 1–19.
47. Sant, G.; Weiss, J. Applications that require a correction before the maturity concept is applied. In Proceedings of the International Conference on Microstructure Related Durability of Cementitious Composites, Nanjing, China, 13–15 October 2008.
48. Poole, J.L.; Riding, K.A.; Folliard, K.J.; Juenger, M.C.; Schindler, A.K. Methods for calculating activation energy for Portland cement. *Aci. Mater. J.* **2007**, *104*, 86.
49. McLachlan, D.S.; Blaszkiewicz, M.; Newnham, R.E. Electrical resistivity of composites. *J. Am. Ceram. Soc.* **1990**, *73*, 2187–2203. [CrossRef]
50. McLachlan, D.S.; Rosenbaum, R.; Albers, A.; Eytan, G.; Grammatica, N.; Hurvits, G.; Pickup, J.; Zaken, E. The temperature and volume fraction dependence of the resistivity of granular Al-Ge near the percolation threshold. *J. Phys. Condens. Matter* **1993**, *5*, 4829–4842. [CrossRef]
51. Oh, B.H.; Jang, S.Y. Prediction of diffusivity of concrete based on simple analytic equations. *Cem. Concr. Res.* **2004**, *34*, 463–480. [CrossRef]
52. Cui, L.; Cahyadi, J.H. Permeability and pore structure of OPC paste. *Cem. Concr. Res.* **2001**, *31*, 277–282. [CrossRef]
53. Castro, J.; Spragg, R.; Kompare, P. *Portland Cement Concrete Pavement Permeability Performance*; Purdue University: West Lafayette, IN, USA, 2010.

54. Backe, K.R.; Lile, O.B.; Lyomov, S.K. Characterising Curing Cement Slurries by Electrical Conductivity. In Proceedings of the SPE Western Regional Meeting, Bakersfield, CA, USA, 10–13 May 1998; Society of Petroleum Engineers: Richardson, TX, USA, 1998.
55. Bentz, D.P. A virtual rapid chloride permeability test. *Cem. Concr. Compos.* **2007**, *29*, 723–731. [CrossRef]
56. Snyder, K.A.; Feng, X.; Keen, B.D.; Mason, T.O. Estimating the electrical conductivity of cement paste pore solutions from OH−, K+ and Na+ concentrations. *Cem. Concr. Res.* **2003**, *33*, 793–798. [CrossRef]
57. Estimation of Pore Solution Conductivity. Available online: http://concrete.nist.gov/poresolncalc.html (accessed on 24 July 2020).
58. Oh, B.H.; Cha, S.W. Nonlinear analysis of temperature and moisture distributions in early-age concrete structures based on degree of hydration. *Mater. J.* **2003**, *100*, 361–370. [CrossRef]
59. Bentz, D.P.; Jensen, O.M.; Coats, A.M.; Glasser, F.P. Influence of silica fume on diffusivity in cement-based materials: I. experimental and computer modeling studies on cement pastes. *Cem. Concr. Res.* **2000**, *30*, 953–962. [CrossRef]
60. Ye, G. Percolation of capillary pores in hardening cement pastes. *Cem. Concr. Res.* **2005**, *35*, 167–176. [CrossRef]
61. Bejaoui, S.; Bary, B. Modeling of the link between microstructure and effective diffusivity of cement pastes using a simplified composite model. *Cem. Concr. Res.* **2007**, *37*, 469–480. [CrossRef]
62. Nokken, M.R.; Hooton, R.D. Using pore parameters to estimate permeability or conductivity of concrete. *Mater. Struct.* **2007**, *41*, 1. [CrossRef]
63. Coverdale, R.T.; Christensen, B.J.; Mason, T.O.; Jennings, H.M.; Garboczi, E.J. Interpretation of the impedance spectroscopy of cement paste via computer modelling. *J. Mater. Sci.* **1994**, *29*, 4984–4992. [CrossRef]
64. Bentz, D.P.; Garboczi, E.J. Percolation of phases in a three-dimensional cement paste microstructural model. *Cem. Concr. Res.* **1991**, *21*, 325–344. [CrossRef]
65. Garboczi, E.J.; Bentz, D.P. Computer simulation of the diffusivity of cement-based materials. *J. Mater. Sci.* **1992**, *27*, 2083–2092. [CrossRef]
66. Isichenko, M. Percolation, statistical topography, and transport in random media. *Rev. Mod. Phys.* **1992**, *64*, 961–1043. [CrossRef]
67. Neithalath, N.; Persun, J.; Manchiryal, R.K. Electrical conductivity based microstructure and strength prediction of plain and modified concretes. *Int. J. Adv. Eng. Sci. Appl. Math.* **2010**, *2*, 83–94. [CrossRef]



© 2020 by the authors. Licensee MDPI, Basel, Switzerland. This article is an open access article distributed under the terms and conditions of the Creative Commons Attribution (CC BY) license (http://creativecommons.org/licenses/by/4.0/).